

Dynamic Relationship Between Oil Temperature and BGCI in Bell 407 Helicopter: A Cointegration and Autoregressive Distributed Lag Approach

Lotfi Saidi^{1,2,4}, Eric Bechhofer³, and Mohamed Benbouzid⁴

¹University of Sousse, Higher School of Sciences and Technology of Hammam Sousse, Sousse 4011, Tunisia

²University of Tunis, - Laboratory of Signal Image and Energy Mastery (SIME), LR 13ES03, ENSIT Tunis 1008, Tunisia;

lotfi.saidi@esst.rnu.tn

³Green Power Monitoring Systems, LLC, VT 05753, USA

eric@gpms-vt.com

⁴University of Brest, UMR CNRS 6027 IRDL, 29238 Brest, France

mohamed.benbouzid@univ-brest.fr

ABSTRACT

The primary objective of this study was to investigate the dynamic relationship between oil temperature and the Bearing Gearbox Condition Indicator (BGCI) values of the Bell 407 helicopter. The study aims to simplify the fault diagnosis process by proposing a method that utilizes only one vibration sensor and one temperature sensor per bearing. To achieve this goal, we employ robust econometric tools, such as unit root tests, cointegration tests, and Autoregressive Distributed Lag (ARDL) models, for both long-run and short-run estimates. Our findings indicate that the variable temperature tends to converge to its long-run equilibrium path in response to changes in other variables. The results of the ARDL analysis confirmed that spectral kurtosis, inner race, cage, and ball energy significantly contributed to the increase in temperature. Furthermore, we utilized the Impulse Response Function (IRF) to trace the dynamic response paths of the shocks to the system. The identification of a cointegrating relationship between oil temperature and BGCI values suggests a practical and significant connection that can potentially be used to predict hazardous changes in oil temperature using BGCI values, which is an important implication for enhancing the safety and reliability of helicopter operations.

The study presents a promising direction for condition

monitoring (CM) in rotating machinery, emphasizing the potential of integrating temperature data to simplify the diagnostic process while still achieving reliable results.

1. INTRODUCTION

The oil temperature significantly affects the bearing performance, lubrication effectiveness, wear rate, and overall operational reliability. Effective thermal management is crucial for gas foil bearings (GFBs) in rotorcraft. High temperatures can lead to increased viscosity of lubricants, reducing their effectiveness and potentially causing bearing hardening and failure (Hechifa, Lakehal, Nanfak, Saidi, Labiod, Kelaiaia, & Ghoneim, 2024).

Various studies have highlighted the critical relationship between temperature and bearing functionality, emphasizing the need for effective thermal management. Increased oil temperature reduces viscosity, leading to inadequate lubrication and higher friction between the mating surfaces, which can result in catastrophic failure, especially under extreme temperature conditions where material performance is critical (Chen, Guan, Cai & Li, 2022), (Soomro, Muhammad, Mokhtar, Saad, Lashari, Hussain, & Palli, 2024), (Saidi, & Benbouzid, 2021).

In rolling bearings, optimal temperature ranges (40°C-60°C) are crucial for effective tribofilm formation, which protects the bearing against wear (Zhao, Hou, Li, Zhang, & Zhu, 2022), (Rosenkranz, Richter, Jacobs, Mikitisin, Mayer, Stratmann, & König, 2021), (Saidi, Ali, Bechhofer & Benbouzid, 2017). The shearing of an oil film generates

Lotfi Saidi et al. This is an open-access article distributed under the terms of the Creative Commons Attribution 3.0 United States License, which permits unrestricted use, distribution, and reproduction in any medium, provided the original author and source are credited.

<https://doi.org/10.36001/IJPHM.2025.v16i1.4233>

heat, which can elevate temperatures within the bearing system, adversely affecting the lubrication performance (Zhang, Tong, & Yin, 2020). A thermos-hydrodynamic lubrication model indicates that the temperature distribution is influenced by circumferential velocity and oil-film thickness, with higher temperatures occurring at minimum film thickness (Zhang, Tong, & Yin, 2020).

The relationship between oil temperature and BGCI values is crucial for assessing the health of helicopter main gearboxes. Monitoring systems like Health Usage Monitoring Systems (HUMS), utilize vibration signatures to detect faults (Zhang, Tong, & Yin, 2020), (Zhang, Jiang, Wu, & Ying, 2012). Oil temperature is a key parameter that affects gearbox health (Bouhadra, & Forest, 2024). Data analysis and artificial intelligence tools are employed to monitor the lubrication and cooling systems of modern helicopters (Li, Li, & Yu, 2019). Additionally, the vibration signatures of damaged components, like bearings, are used as condition indicators, which can vary based on the system design and operating conditions (Koizumi, & Kogiso, 2024) and oil temperature. The use of advanced signal processing tools can help extract bearing fault signatures from vibration signals, thereby enhancing fault detection capability (Ismail, Saidi, Sayadi, & Benbouzid, 2020), (Dass, Gunakala, Comissiong, Azamathulla, Martin, & Ramachandran, 2024), (Babay, Saidi, Bechhofer, & Benbouzid, 2024), (Bechhofer, Schlanbusch, & Waag, 2016), (Saidi, & Benbouzid, 2021). Overall, integrating oil temperature monitoring and bearing condition indicators can provide a comprehensive approach to ensuring the safety and reliability of helicopter gearboxes.

(Tabrizi, Al-Bugharbee, Trendafilova, & Garibaldi, 2017) proposed a novel combined method for fault detection in rolling bearings based on cointegration for the development of fault features that are sensitive to the presence of defects but insensitive to changes in operational conditions.

According to (Zhang, Jiang, Wu, & Ying, 2012), the root cause of high oil temperatures is improper selection of lubricating oil and serious solid particle pollution. Oil analysis techniques are also used to monitor oil working conditions, prevent mechanical failure, and extend the machine's life.

In (Bouhadra, & Forest, 2024), a new diagnostic method based on modulation signal bi-spectrum (MSB) analysis is proposed, which shows that the amplitudes coupled between the fault frequency and epicycle carrier frequency can provide more deterministic information regarding bearing vibrations.

(Li, Li, & Yu, 2019) introduced a health indicator based on cointegration for the run-to-failure process that can depict different run-to-failure data in a unified manner. Through the cointegration test, the study found a certain degree of cointegration between energy and complexity features,

leading to the development of a novel health indicator. The indicator exhibits "two-stage" characteristics, with a zero-line stage followed by a quickly raising stage resembling an exponential function, making it more suitable for an exponential degradation model than the root mean square (RMS).

(Koizumi, & Kogiso, 2024) proposed an improved deep deterministic policy gradient algorithm with a Convolutional Neural Network Long-Short Time Memory (CNN-LSTM) basic learner that can extract the complex relationship between oil temperature and working conditions. A multi-critic network structure was adopted to address inaccurate Q-value estimation.

In (Wu, Kobayashi, Sun., Jen, Sammut, Bird, & Mrad, 2011), the effect of oil and grease on component performance and fault detection was examined in four different aircraft wetted-component case studies, which aimed to improve performance by examining the effect that oil and greases have on components.

(Zhu, Yoon, He, Qu, & Bechhofer, 2013) formed a study group to improve the maintenance strategy of the S61-A4 helicopter fleet in the Malaysian Armed Forces (MAF). The strategy consisted of a structured approach for the reassessment and redefinition of suitable maintenance actions for the main rotor gearbox. In n (Xu, Li, Chen, Wang, Yang, & Yang, 2021), the influence of a dynamic wear model considering the tooth contact flash temperature on the dynamic characteristics of a gear-bearing system was studied, and the effects of the initial wear, friction factors, and damping ratio on the system response were studied.

For CM and defect detection in electromechanical complex systems, cointegration, a methodological approach initially conceived within the domain of (Shafique, Azam, Rafiq, & Luo, 2021), (Ouni, & Ben Abdallah, 2024), has been appropriated for CM as a viable data-driven strategy to mitigate or adjust for pervasive long-term trends induced by the influences of environmental and operational variability present in the observed data.

To overcome the high-temperature bearings problem, advanced materials, such as ceramic matrix composites, are being developed to withstand extreme temperatures without adverse effects, ensuring reliability in harsh conditions (Chen, Guan, Cai & Li, 2022), (Soomro, Muhammad, Mokhtar, Saad, Lashari, Hussain, & Palli, 2024), (Zhao, Hou, Li, Zhang, & Zhu, 2022). While advancements in lubrication systems and materials are promising, the inherent risks of inadequate lubrication remain a critical concern for helicopter safety, necessitating ongoing research and development in this area.

Traditional vibration-based CM for rotating machines, especially those with multiple bearings like turbo-generator sets, is complex and requires extensive data collection. This complexity arises from needing multiple sensors at each

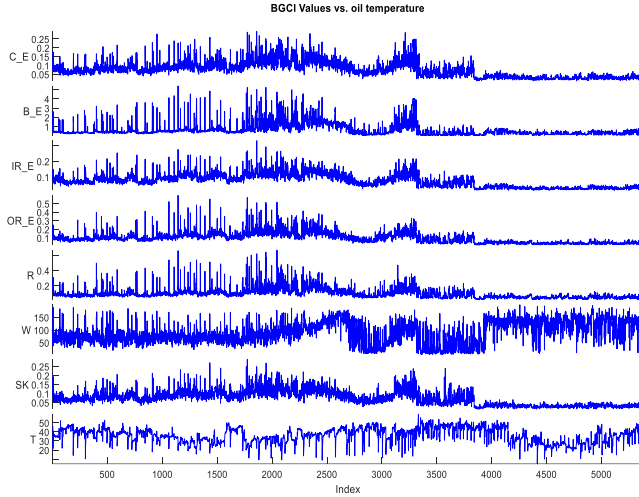


Figure 1. Oil temperature and BGCI values of the Bell 407 helicopter, from top to bottom: Cage Energy (C_E), Ball Energy (B_E), Inner Race Energy (IR_E), Outer Race Energy (OR_E), $1/Rev$ (R), Whip (W), Spectral Kurtosis (SK), and Temperature (T)

bearing location, making fault diagnosis challenging even for experienced analysts. The study aims to simplify the fault diagnosis process by proposing a method that utilizes only one vibration sensor and one temperature sensor per bearing. This approach is intended to reduce the data collection burden while maintaining effective monitoring capabilities.

The present study investigates the dynamic relationship between oil temperature and BGCI in a Bell 407 helicopter. To achieve this goal, we employ robust econometric tools, such as unit root tests, cointegration tests, and ARDL models, for both long- and short-run estimates. We utilized the Dumitrescu Hurlin (Dumitrescu, & Hurlin, 2012) panel causality tests to confirm the causal relationships between the variables. In summary, the contributions of this paper lie in its innovative approach to simplifying fault diagnosis, integrating temperature data, applying cointegration tests, and ARDL models for enhanced analysis, providing experimental validation, and offering practical solutions for industrial applications. These contributions collectively advance the field of CM for rotating machinery.

This paper's remaining structure is outlined as follows: Section 2 describes the data collection. Section 3 presents the methodology. Section 4 shows the results. Finally, Section 5 concludes this paper.

2. HUMS DATA COLLECTION

The HUMS was developed to provide a holistic measure of aircraft health by providing automated flight data monitoring, rotor track and balance, engine performance monitoring, and drivetrain diagnostics/prognostics. The system incorporates ten smart accelerometers to collect and

process vibration data into condition indicators. The accessory drive sensor monitors this study's duplex bearing. This bearing supports the accessory drive's hydraulic pump, which operates at 4450 RPM. The sensor's sample rate was 46875 samples per second (sps) for 2 s. The sensor performed an envelope (Abboud, Antoni, Sieg-Zieba, & Eltabach, 2017) in a window from 9 to 13 kHz. The system was designed to acquire data every four minutes depending on the aircraft regime. That is, after four minutes, if the aircraft is relatively straight and level, the data are captured. If the aircraft is manoeuvring, the acquisition is delayed until the aircraft is again straight and level.

The criteria for determining when the aircraft is considered straight and level are based on the aircraft's pitch and roll angles, which are monitored using onboard sensors. Specifically, we define "straight and level" as maintaining a pitch angle within ± 2 degrees and a roll angle within ± 3 degrees of the horizontal plane. This ensures that the aircraft is in a stable flight condition, minimizing the effects of maneuvers on the data collected. Furthermore, the data acquisition system is programmed to delay data capture if the aircraft exceeds these thresholds, ensuring that only stable flight conditions are recorded.

Figures 1 show the oil temperature and BGCI of the Bell 407 helicopter. Here is important information. The gearbox oil was replaced in 2020, on December 22. It was hypothesized that the oil was contaminated with wear debris from the gearbox, which was causing the ball energy to increase (Fig.2). The CI energy then went down. However, we can see that from April 6, 2021, the fault started to propagate. The bearing was replaced on June 11, 2021.

While the figures 1, and 2 may not explicitly show the dates, they illustrate trends in oil temperature and BGCI values. The increase in ball energy can be inferred from the data trends leading up to the replacement date. The figures likely depict the changes in these indicators over time, allowing readers to visualize the relationship between the fault conditions and the timing of the bearing replacement.

The other way to look at this is the "peak" energy only seen at the start of a flight, so on the ground. That would be another avenue of research is to look at the regime in which the analysis was taken.

3. METHODOLOGY

This study aimed to analyze the dynamic effects of cage, ball, inner, and outer race energy, $1/Rev$, whip, and spectral kurtosis on the temperature.

The general form of the empirical equation is as follows:

$$T_t = f(C_{Et}, B_{Et}, IR_{Et}, OR_{Et}, R_t, W_t, SK_t) \quad (1)$$

Here, T is the temperature, C_E is the Cage Energy, B_E denotes Ball Energy, IR_E represents Inner Race Energy, OR_E

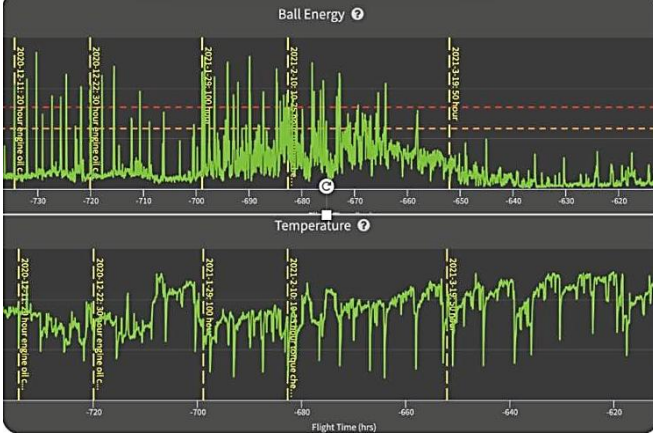


Figure 2. Regression of the CI data based on temperature against ball energy.

represents Outer Race Energy, R represents $1/Rev$, W represents whip, SK represents Spectral Kurtosis, and t denotes acquisition time.

The BGCI serves as a vital, integrative metric for assessing the health and operational performance of bearing gearbox. In this study, BGCI is meticulously constructed from key parameters, including temperature, C_E , B_E , IR_E , OR_E , R , W and SK , as outlined in Equation 1. Together, these variables capture the intricate dynamics and condition of the bearing gearbox components, delivering a holistic perspective on system integrity. By incorporating BGCI into advanced econometric modeling frameworks, this study significantly enhances the reliability and safety of helicopter operations. This innovative integration not only refines maintenance strategies but also sets a benchmark for the application of condition-monitoring metrics in high-stakes aerospace systems.

To examine long-run linkages between variables, we employed the following equation derived from Eq. (1):

$$T_t = \alpha_0 + \alpha_1 C_{Et} + \alpha_2 B_{Et} + \alpha_3 IR_{Et} + \alpha_4 OR_{Et} + \alpha_5 R_t + \alpha_6 W_t + \alpha_7 SK_t + \varepsilon_t \quad (2)$$

The estimated econometric model presented above is not in linear form, does not present consistent results, and is not helpful to the decision-making process. To address this issue, we transformed all variables into natural logarithms to analyze the relationships between the dependent and independent variables. Using a log-linear specification model offers several advantages in terms of achieving consistent and robust empirical findings (Shafique, Azam, Rafiq, & Luo, 2021), (Ouni, & Ben Abdallah, 2024). Therefore, the log-linear form is given by Eq. (3):

$$\begin{aligned} \ln T_t = & \alpha_0 + \alpha_1 \ln C_{Et} + \alpha_2 \ln B_{Et} + \alpha_3 \ln IR_{Et} \\ & + \alpha_4 \ln OR_{Et} + \alpha_5 \ln R_t + \alpha_6 \ln W_t \\ & + \alpha_7 \ln SK_t + \varepsilon_t \end{aligned} \quad (3)$$

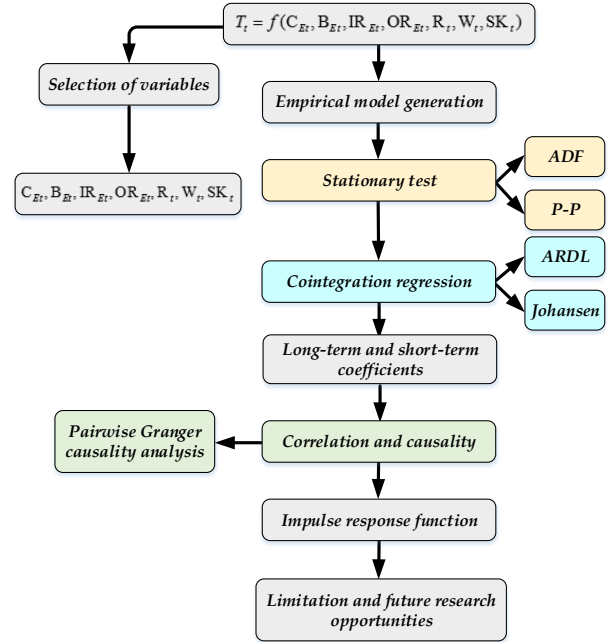


Figure 3. Flowchart of analytical techniques used in the study

Where $\ln T$ is the natural logarithm of temperature, $\ln C_{Et}$ is the natural logarithm of the C_E , $\ln B_{Et}$ is the natural logarithm of B_E , $\ln IR_{Et}$ is the natural logarithm of IR_E , $\ln OR_{Et}$ is the natural logarithm of OR_E , $\ln R_t$ is the natural logarithm of Rev , $\ln W_t$ is the natural logarithm of whip, and $\ln SK_t$ is the natural logarithm of SK . α_0 represents the constant term. α_1 , α_2 , α_3 , α_4 , α_5 , α_6 , and α_7 are the slope coefficients of the explanatory variables. ε_t represents the error term.

Note that applying log transformation to variables that may take on zero or negative values can lead to undefined results. In our study, we took this concern into account by implementing a careful pre-processing step for the BGCI values. Specifically, we ensured that all BGCI values were positive before applying the log transformation.

To achieve this, we utilized a small constant (e.g., adding 1) to all BGCI values to shift the entire dataset into the positive range. This adjustment allows us to maintain the integrity of the data while still benefiting from the linearization properties of the log transformation. Additionally, we conducted sensitivity analyses to confirm that this transformation did not significantly alter the relationships we aimed to study.

A cointegration-based computation procedure, consisting of three stages, was developed for this purpose. The methodology presented in the paper is described in a general manner in Figure 3, with specific steps outlined for the application of econometric tools such as ARDL models, cointegration tests, and IRF. Indeed, in the first stage, a

cointegration model of the monitored bearing gearbox is established using a set of condition indicator values. This model has the role of a bearing oil temperature monitoring model. In the second stage, the stationarity test was carried out. In the third stage, the cointegration procedure is deployed. The next stage used the ARDL model to examine the long and short-term relationships between the explanatory variables and the temperature. The correlation and causality tests were carried out in the fourth stage. In the last stage, we employed the IRF to measure the effects of shocks from independent variables on the dependent variable.

3.1. Estimation Procedures

The first step in our analysis was to employ unit root tests to verify the stationarity of all variables. We utilized the standard unit root tests such as the Augmented Dickey-Fuller (ADF) test (Ouni, & Ben Abdallah, 2024) and the Phillips-Perron (PP) test (Phillips, 1988), (Dickey, & Fuller, 1979). These tests support the null hypothesis that a series possesses a unit root (indicating non-stationarity), while the alternative hypothesis suggests stationarity. The ADF unit root test was used to assess the presence of autocorrelation in the series, and the PP unit root test was used to examine heteroscedasticity in the time series. A time series is considered non-stationary if one or more of its moments (mean, variance, or covariance) are not time-independent. A non-stationary series with a stochastic unit root must be differenced once to achieve stationarity. Before exploring cointegration analysis, it is imperative to empirically establish the integration process.

The empirical equation for the ADF unit root test is given by Eq. (4):

$$\Delta Y_t = \beta_0 + Y_{t-1} + \sum_{i=1}^m d_i \Delta Y_{t-i} + \mu_t \quad (4)$$

Where Δ represents the first difference operator, μ_t denotes the error term, β_0 is the intercept term associated with the equations, m indicates the number of lags of the specific variable in the model, and t represents the time measure.

The empirical equation for the PP unit root test can be expressed in Eq. (5):

$$\Delta Y_t = \beta + \theta \times Y_{t-1} + \mu_t \quad (5)$$

The long-term relationships among temperature, cage, ball energy, inner race energy, outer race energy, Rev , whip, and spectral kurtosis are investigated using the ARDL and Johansen-Juselius cointegration tests.

The Johansen-Juselius (Johansen, & Juselius, 1990) cointegration approach is employed to examine long-run relationships among variables. The Johansen-Juselius cointegration technique is constructed on λ_{trace} and λ_{max} statistics. Trace statistics investigates the null hypothesis of

cointegrating relations against the alternative of N cointegrating relations and is computed as:

$$\lambda_{trace} = N \sum_{i=r+1}^n \log(1 - \lambda_i) \quad (6)$$

Where N is the number of observations.

The maximum eigenvalue statistics test the null hypothesis of r cointegrating relations with:

$$\lambda_{max} = N \log(1 - \lambda_r + 1) \quad (7)$$

The ARDL model introduced by (Pesaran, Shin, & Smith, 2001) examines the existence of long-run and short-run relationships between the variables under examination. This method offers several advantages over traditional cointegration tests. Firstly, it addresses endogeneity issues by accommodating appropriate variable lag lengths for both independent and dependent (Narayan, 2005). Second, it can handle a mixture of stationary variables such as $I(0)$ and $I(1)$ but not $I(2)$ (Pesaran, Shin, & Smith, 2001). Third, the ARDL bound testing approach demonstrated improved efficiency and robustness, effectively mitigating issues related to autocorrelation. Moreover, the ARDL model allows for varying lag lengths, thereby enhancing its flexibility and enabling the estimation of both long-term and short-term dynamics through an error correction model (ECM). The ARDL model is defined as follows:

$$\begin{aligned} \Delta Ln T_t = & \alpha_0 + \sum_{k=1}^n \alpha_{1k} \Delta Ln T_{t-k} + \sum_{k=1}^n \alpha_{2k} \Delta Ln C_{Et-k} \\ & + \sum_{k=1}^n \alpha_{3k} \Delta Ln B_{Et-k} + \sum_{k=1}^n \alpha_{4k} \Delta Ln IR_{Et-k} \\ & + \sum_{k=1}^n \alpha_{5k} \Delta Ln OR_{Et-k} + \sum_{k=1}^n \alpha_{6k} \Delta Ln R_{t-k} \\ & + \sum_{k=1}^n \alpha_{7k} \Delta Ln W_{t-k} + \sum_{k=1}^n \alpha_{8k} \Delta Ln SK_t \\ & + \delta_1 Ln T_{t-1} + \delta_2 Ln C_{Et-1} + \delta_3 Ln B_{Et-1} \\ & + \delta_4 Ln IR_{Et-1} + \delta_5 Ln OR_{Et-1} + \delta_6 Ln R_{t-1} \\ & + \delta_7 Ln W_{t-1} + \delta_8 Ln SK_{t-1} + \varepsilon_t \end{aligned} \quad (8)$$

After obtaining long-run coefficients from Eq. (8), we use the ECM described in Eq. (9) to analyze short-term relationships.

$$\begin{aligned} \Delta Ln T_t = & \alpha_0 + \sum_{k=1}^n \alpha_{1k} \Delta Ln T_{t-k} + \sum_{k=1}^n \alpha_{2k} \Delta Ln C_{Et-k} \\ & + \sum_{k=1}^n \alpha_{3k} \Delta Ln B_{Et-k} + \sum_{k=1}^n \alpha_{4k} \Delta Ln IR_{Et-k} \\ & + \sum_{k=1}^n \alpha_{5k} \Delta Ln OR_{Et-k} + \sum_{k=1}^n \alpha_{6k} \Delta Ln R_{t-k} \\ & + \sum_{k=1}^n \alpha_{7k} \Delta Ln W_{t-k} + \sum_{k=1}^n \alpha_{8k} \Delta Ln SK_t \\ & + \gamma ECM_{t-1} + \varepsilon_t \end{aligned} \quad (9)$$

Where the difference operator is defined by Δ , the optimal lag length of the variables is denoted by n , the error correction term ECM_{t-1} coefficient is indicated by γ , and the residual error term is presented by ε_t . Under the ARDL framework, the null hypothesis of no cointegration; $H_0 = \delta_1 = \delta_2 = \delta_3 = \delta_4 = \delta_5 = \delta_6 = \delta_7 = \delta_8 = 0$ against the alternative hypothesis of cointegration $H_1 = \delta_1 \neq \delta_2 \neq \delta_3 \neq \delta_4 \neq \delta_5 \neq \delta_6 \neq \delta_7 \neq \delta_8 \neq 0$ is tested by taking the F-statistics used by Narayan (2005) (Narayan, 2005).

When the computed F-value exceeds the upper bound, cointegration is indicated; conversely, when the computed F-value is below the lower bound, no cointegration is indicated. However, if the F-value falls between the upper and lower critical values, the decision of cointegration is inconclusive. Additionally, a significant error correction term suggests a long-term relationship between variables.

Then, we examined the causal relationship between temperature and other variables using the Dumitrescu and Hurlin test (Dumitrescu, & Hurlin, 2012), which is a simplified version of Granger's (Granger, 2001) non-causality test. We chose this test because it considers two different types of heterogeneity: one in the regression model used to evaluate Granger causality and another in the causality relationship itself. In our analysis, we employed the linear model shown in Eq. (10):

$$Y_{it} = a_i + \sum_{i=1}^k \gamma_i^{(k)} Y_{it-k} + \sum_{i=1}^k \beta_i^{(k)} X_{it-k} + \varepsilon_{it} \quad (10)$$

Where γ_i represents the slope coefficients, a_i represents the cross-sectional unit, and k represents the lag length. In this context, the null hypothesis suggests that there is no causal relationship in at least one cross-sectional unit. To test this null hypothesis, we used the Z-bar statistics (\bar{Z}) and W-bar statistic (\bar{W}) tests, which can be computed as follows:

$$\bar{W} = \frac{1}{N} \sum_{i=1}^N W_i \quad (11)$$

$$\bar{Z} = \sqrt{\frac{N}{2K}} (\bar{W} - K) \quad (12)$$

Innovation accounting is employed to analyze the relationship between selected variables in a given dataset. This method uses the IRF to visually demonstrate how shocks in one variable affect others, altering their magnitudes over time. The IRF highlights the impacts of these shocks on both current and future values of the variables involved. Specifically, a standard error shock in one variable during the period 't+s' may positively, negatively, or bidirectionally influence another variable 'j' at period 't'. This relationship can be mathematically expressed as follows in Eq. (13):

$$\psi_s = \frac{\varphi Y_{i,t+s}}{\varphi \mu_{j,t}} \quad (13)$$

Where Y represents the dependent variables, and μ is the forecast error term.

4. RESULTS

4.1. Unit root analysis

To study the relationship between temperature, cage, ball energy, inner race energy, outer race energy, *Rev*, whip, and spectral kurtosis, we verified the presence of unit roots in the variables using ADF and PP tests. Table 1 presents the outcomes of the ADF and PP tests. This indicates that all variables (LnT , LnC_E , LnB_E , $LnOR_E$, LnR , LnW , $LnSK$) are stationary at this level, except the variable $LnIR_E$, which is stationary at the first difference. Therefore, some variables are $I(0)$ and others are $I(1)$. It is concluded that the variables used in this study have a mixed order of integration, as evidenced by both the ADF and PP unit root tests.

4.2. Cointegration tests

After confirming the integration order of the variables, this study employs the ARDL bounds model and the Johansen-Juselius cointegration test to investigate cointegration among the variables under examination. The results of the ARDL bound testing are presented in Table 2. When we analyzed the ARDL model with LnT as the dependent variable, we found evidence of cointegration in the series under consideration. This conclusion was drawn by observing that both the upper and lower bound critical values were well below the estimated F-statistic (5.534). Thus, we reject the null hypothesis of no cointegration, suggesting the presence of a long-term relationship between variables.

The results of the Johansen cointegration test, as shown in Table 3, indicate that both the maximum eigenvalue and trace tests reject the null hypothesis of no cointegration. Specifically, at a 5% significance level, the tests reveal eight cointegrating equations.

4.3. Long-run and short-run analysis

Before applying the ARDL model, it is crucial to select the optimal lag length. Various criteria, such as the Akaike Information Criterion (AIC), Hannan-Quinn (HQ) Information Criterion, and Schwarz-Bayesian Criterion (SBC), help determine the optimal lag length. In this study, the optimal lag length was determined using the AIC criteria. Table 4 presents the results of long- and short-run analysis using the ARDL model.

The speed of ECM_{t-1} of the model satisfies the expected condition of a negative and significant value that corrects the previous period's disequilibrium in the coming period (-0.811). The results show that the variable whip significantly decreases with temperature in both the long and short run. This implies that in the long term (short run), a 1% increase

Variables	ADF		PP	
	Level	Δ	Level	Δ
LnT	-8.460***	-32.875***	-17.104***	-29.324***
LnC_E	-3.619***	-32.923***	-10.094***	-38.303***
LnB_E	-5.725***	-30.881***	-8.831***	-45.706***
LnI_{R_E}	-0.703	-35.604***	-1.153	-37.367***
LnO_{R_E}	-4.548***	-30.650***	-19.252***	-43.162***
LnR	-5.801***	-30.347***	-12.187***	-29.177***
LnW	-5.146***	-25.347***	-17.309***	-36.076***
$LnSK$	-3.817***	-34.203***	-12.572***	-31.278***

Note: *** indicates a 1% level of significance, Δ denotes the first difference

Table 1. Results of unit root tests

in the whip results in a significant decrease in temperature of 0.215% (0.248%).

The direct influence of whip on oil temperature can be attributed to several physical processes:

- Increased Friction: As whip increases, it may lead to greater oscillations and vibrations within the helicopter's components. This can result in increased friction between moving parts, which generates additional heat. The heat generated can subsequently raise the oil temperature.
- Viscosity Changes: Higher temperatures can reduce the viscosity of the oil, leading to less effective lubrication. This can create a feedback loop where increased whip leads to higher temperatures, which in turn affects lubrication efficiency and further exacerbates the heating.
- Intermediate Variables: While the study primarily focuses on the relationship between whip and oil temperature, it is essential to consider potential intermediate variables that could mediate this relationship; namely the condition of bearings can be influenced by both whip and temperature. Increased whip may lead to wear and tear on bearings, which can affect their performance and generate additional heat. In addition, the operational load on the helicopter can also play a role. Under higher loads, the effects of whip may be more pronounced, leading to greater temperature increases.

To provide quantifiable information about how temperature converges to its equilibrium path, we can refer to the results obtained from the ARDL model analysis. Specifically, the ECMt-1 demonstrated a significant negative coefficient of -0.811, indicating a strong adjustment mechanism in the model. This value suggests that approximately 81.1% of the disequilibrium from the previous period is corrected in the current period. This suggests a strong tendency for the temperature variable to return to its long-run equilibrium following shocks from other variables. Additionally, the analysis revealed that a 1% increase in the variable "whip" leads to a significant decrease in temperature by 0.215% in the long run and 0.811% in the short run, further illustrating the dynamic relationship and responsiveness of temperature to changes in other influencing factors. A coefficient of -0.811 suggests that if there is a shock to the system, it will take less than a year (approximately 1.23 periods, given the

Estimated model	F-statistics	
$LnT = f(LnC_{Et}, LnB_{Et}, LnI_{REt}, LnO_{REt}, LnR_t, LnW_t, LnSK_t)$	5.534*	
	Lower bound	Upper bound
Significance level		
1%	3.09	3.86
5%	2.93	3.83
10%	2.101	3.869

Note: * indicates a 10% level of significance.

Table 2: ARDL Bound tests for cointegration

	Eigenvalue	Trace Statistic	Critical value 0.05	Prob**
None *	0.149	3380.233	159.529	0.000
At most 1 *	0.135	2507.699	125.615	0.000
At most 2 *	0.110	1721.344	95.753	0.000
At most 3 *	0.087	1090.921	69.818	0.000
At most 4 *	0.056	596.760	47.856	0.000
At most 5 *	0.025	286.123	29.797	0.000
At most 6 *	0.022	147.548	15.494	0.000
At most 7 *	0.004	23.174	3.841	0.000

Note: Trace test indicates 8 cointegrating eqn(s) at the 0.05 level. Further, *** denotes rejection of the hypothesis at the 0.05 level.

Table 3. Johansen cointegration test.

quarterly data) for the system to return to equilibrium. This rapid adjustment is particularly important in applications such as helicopter maintenance, where timely responses to changes in oil temperature can prevent potential failures.

These metrics provide a clearer understanding of how temperature converges to its equilibrium path in response to variations in other variables.

The variable Rev has a negative and significant impact on temperature in both the long- and short-term. According to these results, a 1% increase in Rev decreased the temperature by 0.219% (0.277%) eventually (short run).

The analysis reveals a statistically significant positive relationship between ball energy and oil temperature. Specifically, a 1% increase in ball energy leads to an estimated increase in oil temperature by 0.112% in the long term and 0.155% in the short term. This indicates that fluctuations in ball energy have an immediate and slightly greater impact on temperature in the short term compared to the long term, underscoring the dynamic influence of ball energy on the thermal state of the system. Such findings highlight the importance of monitoring ball energy as a key condition indicator in predictive maintenance strategies, as sustained increases could contribute to overheating and reduced system efficiency.

Table 4 presents the diagnostic test results of the proposed model. An R^2 value of 0.85 indicates a strong fit of the estimated model. Additionally, tests for serial correlation, heteroscedasticity, Ramsey tests, and normality confirm that

Regressors	Coefficient	t-statistics	Prob
Long-run analysis			
LnW	-0.215	-8.773	0.000***
LnR	-0.219	-6.621	0.000***
$LnOR_E$	-0.178	-4.398	0.000***
$LnSK$	0.025	0.636	0.524
$LnIR_E$	0.193	4.197	0.000***
LnC_E	0.035	0.823	0.410
LnB_E	0.112	3.557	0.000***
Short-run analysis			
ECM_{t-1}	-0.811	-1.470	0.000***
$\Delta(LnW)$	-0.248	-7.787	0.000***
$\Delta(LnR)$	-0.277	-5.673	0.000***
$\Delta(LnOR_E)$	-0.233	-3.477	0.000***
$\Delta(LnSK)$	0.030	0.433	0.664
$\Delta(LnIR_E)$	0.292	3.656	0.000***
$\Delta(LnC_E)$	-0.015	-0.202	0.839
$\Delta(LnB_E)$	0.155	3.772	0.000***
Constant	4.281	0.069	0.000***
Diagnostic tests			
R^2	0.85		
$X^2 ARCH$	0.388 (0.960)		
$X^2 Ramsey$	2.839 (0.213)		
$X^2 LM$	0.352 (0.399)		
$X^2 Normality$	0.144 (0.930)		

Note: *** indicates a 1% significance level.

Table 4. Results of ARDL estimation (LnT is a dependent variable)

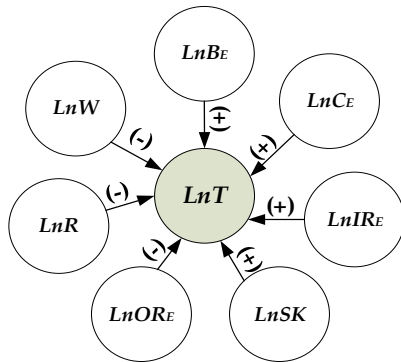


Figure 4. Summary of empirical results

our model is correctly specified and follows normality. Furthermore, these tests confirmed the absence of serial correlation and heteroscedasticity.

Figure 4 presents a summary of empirical results, illustrating the relationships between LnT and several influencing variables. LnB_E , $LnIR_E$, and $LnSK$ positively impact LnT , suggesting that an increase in these factors leads to its growth, while LnW , LnR , and $LnOR_E$ have a negative effect, indicating that their increase hinders LnT . LnC_E has a mixed influence, implying a complex relationship. The diagram effectively visualizes the directional impact of these variables, highlighting key drivers and inhibitors of LnT .

Null hypothesis	F-statistic	Prob
LnW does not Granger cause LnT	8.935	0.0000***
LnT does not Granger cause LnW	9.945	5.E-05***
LnR does not Granger cause LnT	3.223	0.039**
LnT does not Granger cause LnR	5.953	0.002***
$LnOR_E$ does not Granger cause LnT	0.841	0.431
LnT does not Granger cause $LnOR_E$	5.985	0.002***
$LnSK$ does not Granger cause LnT	0.317	0.727
LnT does not Granger cause $LnSK$	6.083	0.002***
$LnIR_E$ does not Granger cause LnT	1.154	0.315
LnT does not Granger cause $LnIR_E$	5.189	0.005***
LnC_E does not Granger cause LnT	0.672	0.510
LnT does not Granger cause LnC_E	3.791	0.022**
LnB_E does not Granger cause LnT	4.412	0.012**
LnT does not Granger cause LnB_E	4.853	0.007***

Note: *, **, and *** indicate 1%, 5%, and 10% levels of significance, respectively.

Table 5. Pairwise Granger causality analysis

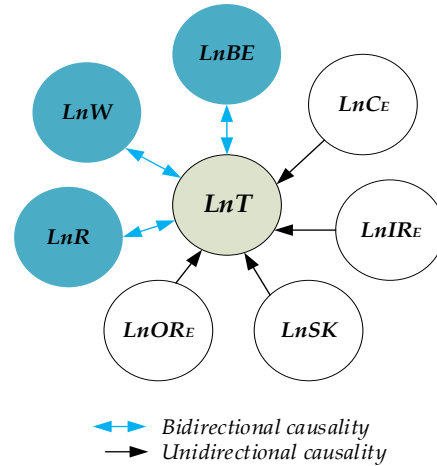


Figure 5. Granger causality results

4.4. Pairwise Granger causality analysis

The relationship between the variables suggests the presence of Granger causality, as determined by the F-statistic. The summary of pairwise Granger causality is provided in Table 5 and Figure 5, which includes the direction of causality between the variables. The results of the pairwise Granger causality tests indicate a unidirectional causality relationship from temperature to outer race energy, spectral kurtosis, inner race energy, and cage. Our findings suggest a bidirectional causal relationship between whip and temperature, Rev and temperature, as well as temperature and ball energy.

4.5. Impulse response function

Understanding the dynamic response of a system to various shocks is a critical aspect of many electromechanical

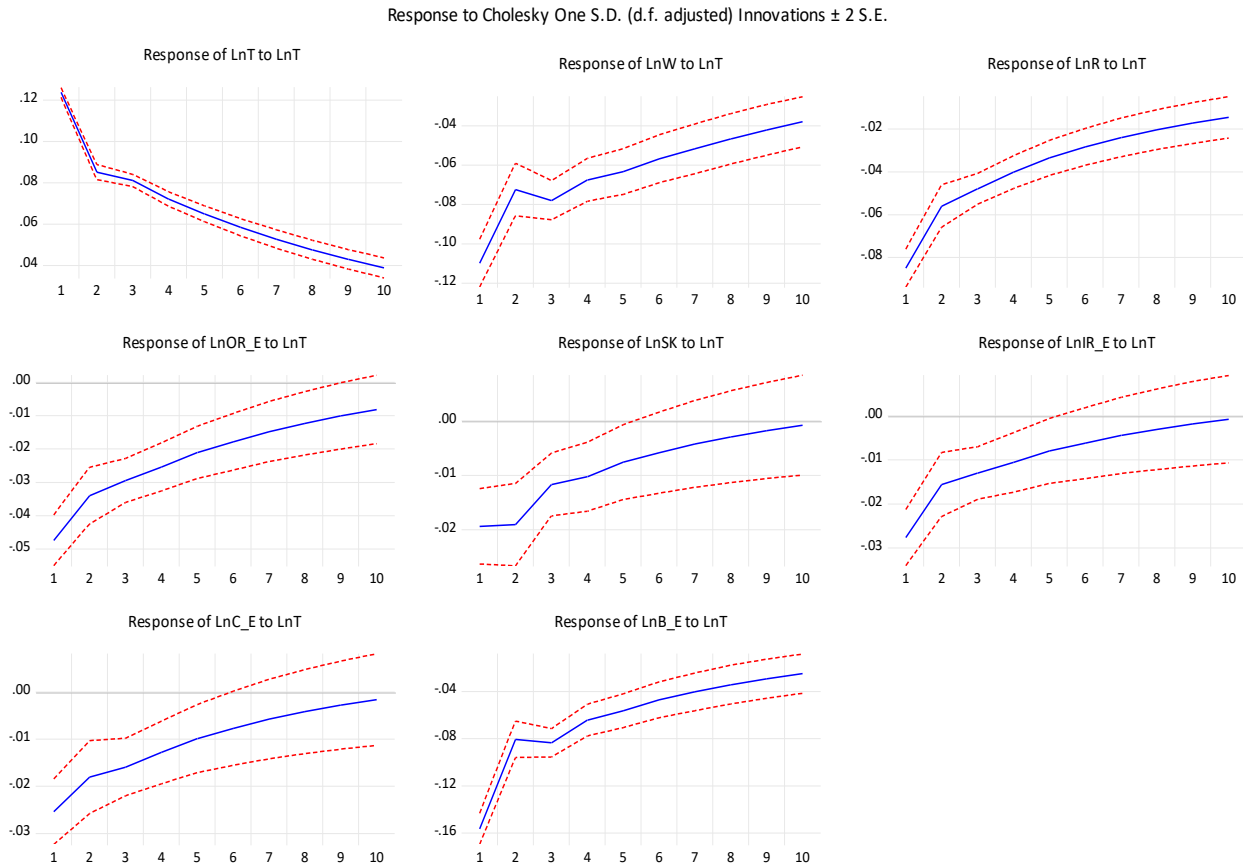


Figure 6. IRFs of the temperature model

process analyses. The IRF is a powerful tool for tracing the temporal evolution of these dynamic responses (GomezGonzalez, Hirs-Garzon, & Uribe Gil, 2020), (Koop, Pesaran, & Potter, 1996). In other words, the IRF plays a crucial role in measuring the impact of shocks from independent variables on the dependent variable. This method allows us to analyze the dynamic interactions among the variables in our model and helps us quantify the effects of these shocks. Figure 6 illustrates the IRFs of the temperature model.

From a theoretical perspective, the long-term effects of demand shocks have been a subject of debate. While traditional approaches suggest that demand shocks may have transitory effects, endogenous growth models suggest that they can have persistent, either positive or negative, impacts in the long run.

5. CONCLUSION

The conclusions drawn from this paper highlight the effectiveness and practicality of the proposed CM method. In this context, the integration of oil temperature monitoring and cointegration analysis offers a promising approach for diagnosing helicopter bearings under varying operational

conditions. This method enhances the reliability of health monitoring systems by combining vibration data with oil temperature metrics, leading to improved safety capabilities. Indeed, this paper employs econometric tools, such as ARDL models and cointegration analysis, to assess both long-run and short-run dynamics in this relationship. The study introduces a novel application of these econometric methods in the field of CM and aims to enhance predictive maintenance strategies for helicopter gearboxes. The paper stands out by applying econometric models, which are not commonly used in the CM community, to analyze rotating machinery data. This approach offers a fresh perspective and could inspire new avenues of research within the field. The findings have potential practical applications, particularly in improving predictive maintenance and monitoring of helicopter gearboxes. The identification of a cointegrated relationship between oil temperature and BGCi values could lead to more effective health monitoring systems.

While the results are promising, one of the challenges noted in the study is the potential overlap between different fault conditions. The study focused on commonly encountered gearbox bearing faults, but it may not encompass all possible fault scenarios that could occur in rotating

machinery in rotorcraft. This limitation could affect the robustness of the proposed diagnostic methods when applied to less common or more complex fault conditions. These factors highlight areas for future research and improvement in the proposed diagnostic methods.

Moreover, the authors suggest that further experimentation on different rigs and with various fault types is necessary to fully validate the method's effectiveness and explore its potential for broader industrial applications.

References

- Hechifa, A., Lakehal, A., Nanfak, A., Saidi, L., Labiod, C., Kelaiaia, R., & Ghoneim, S. S. (2024). Improved intelligent methods for power transformer fault diagnosis based on tree ensemble learning and multiple feature vector analysis. *Electrical Engineering*, 106(3), 2575-2594.
- Chen, B., Guan, X., Cai, D., & Li, H. (2022). Simulation on thermal characteristics of high-speed motorized spindle. *Case Studies in Thermal Engineering*, 35, 102144.
- Soomro, A. A., Muhammad, M. B., Mokhtar, A. A., Saad, M. H. M., Lashari, N., Hussain, M., & Palli, A. S. (2024). Insights into modern machine learning approaches for bearing fault classification: A systematic literature review. *Results in Engineering*, 102700.J.
- Saidi, L., & Benbouzid, M. (2021). Prognostics and health management of renewable energy systems: state of the art review, challenges, and trends. *Electronics*, 10(22), 2732.
- Zhao, J., Hou, L., Li, Z., Zhang, H., & Zhu, R. (2022). Prediction of tribological and dynamical behaviors of spur gear pair considering tooth root crack. *Engineering Failure Analysis*, 135, 106145.
- Rosenkranz, L., Richter, S., Jacobs, G., Mikitisin, A., Mayer, J., Stratmann, A., & König, F. (2021). Influence of temperature on wear performance of greases in rolling bearings. *Industrial Lubrication and Tribology*, 73(6), 862-871.
- Saidi, L., Ali, J. B., Bechhoefer, E., & Benbouzid, M. (2017, October). Particle filter-based prognostic approach for high-speed shaft bearing wind turbine progressive degradations. In *IECON 2017-43rd Annual Conference of the IEEE Industrial Electronics Society* (pp. 8099-8104). IEEE.
- Zhang, G., Tong, B., & Yin, Y. (2020). Temperature distribution and heat generating/transfer mechanism of the circular bilayer porous bearing for thermo-hydrodynamic problem. *International Journal of Heat and Mass Transfer*, 149, 119134.
- Ismail, A., Saidi, L., Sayadi, M., & Benbouzid, M. (2020). Remaining useful lifetime prediction of thermally aged power insulated gate bipolar transistor based on Gaussian process regression. *Transactions of the Institute of Measurement and Control*, 42(13), 2507-2518.
- Tabrizi, A. A., Al-Bugharbee, H., Trendafilova, I., & Garibaldi, L. (2017). A cointegration-based monitoring method for rolling bearings working in time-varying operational conditions. *Meccanica*, 52, 1201-1217.
- Zhang, Y. G., Jiang, X. F., Wu, X. W., & Ying, Z. (2012). Diagnosis of High Oil Temperature of the Bearings Based on Oil Analytical Techniques. *Applied Mechanics and Materials*, 224, 119-122.
- Bouhadra, K., & Forest, F. (2024). Knowledge-based and Expert Systems in Prognostics and Health Management: a Survey. *International Journal of Prognostics and Health Management*, 15(2).
- Li, H., Li, Y., & Yu, H. (2019). A novel health indicator based on cointegration for rolling bearings' run-to-failure process. *Sensors*, 19(9), 2151.
- Koizumi, T., & Kogiso, N. (2024). An Effectiveness Evaluation Method Using System of Systems Architecture Description of Aircraft Health Management in Aircraft Maintenance Program. *International Journal of Prognostics and Health Management*, 15(3).
- Dass, T. D., Gunakala, S. R., Comissiong, D., Azamathulla, H. M., Martin, H., & Ramachandran, S. (2024). Investigating journal bearing characteristics incorporating variable viscosity, couple-stress lubricant, slip-velocity, magnetic fluid, and sinusoidal surface-texturing. *Results in Engineering*, 102338.
- Tahmasbi, D., Shirali, H., Souq, S. S. M. N., & Eslampanah, M. (2024). Diagnosis and root cause analysis of bearing failure using vibration analysis techniques. *Engineering Failure Analysis*, 158, 107954.
- Bechhoefer, E., Schlanbusch, R., & Waag, T. I. (2016). Techniques for large, slow bearing fault detection. *International Journal of Prognostics and Health Management*, 7(1).

- Saidi, L., & Benbouzid, M. (2021). Prognostics and health management of renewable energy systems: state of the art review, challenges, and trends. *Electronics*, 10(22), 2732.
- Wu, K. T., Kobayashi, M., Sun, Z., Jen, C. K., Sammut, P., Bird, J., & Mrad, N. (2011). Engine oil condition monitoring using high temperature integrated ultrasonic transducers. *International Journal of Prognostics and Health Management*, 2(2).
- Zhu, J., Yoon, J. M., He, D., Qu, Y., & Bechhoefer, E. (2013). Lubrication oil condition monitoring and remaining useful life prediction with particle filtering. *International Journal of Prognostics and Health Management*, 4, 124-138.
- Xu, J., Li, X., Chen, R., Wang, L., Yang, Z., & Yang, H. (2021). Dynamic characteristics analysis of gear-bearing system considering dynamic wear with flash temperature. *Mathematics*, 9(21), 2739.
- Shafique, M., Azam, A., Rafiq, M., & Luo, X. (2021). Investigating the nexus among transport, economic growth and environmental degradation: Evidence from panel ARDL approach. *Transport Policy*, 109, 61-71.
- Uni, M., & Ben Abdallah, K. (2024). Environmental sustainability and green logistics: Evidence from BRICS and Gulf countries by cross-sectionally augmented autoregressive distributed lag (CS-ARDL) approach. *Sustainable Development*.
- Dumitrescu, E. I., & Hurlin, C. (2012). Testing for Granger non-causality in heterogeneous panels. *Economic modelling*, 29(4), 1450-1460.
- Abboud, D., Antoni, J., Sieg-Zieba, S., & Eltabach, M. (2017). Envelope analysis of rotating machine vibrations in variable speed conditions: A comprehensive treatment. *Mechanical Systems and Signal Processing*, 84, 200-226.
- Dickey, D. A., & Fuller, W. A. (1979). Distribution of the estimators for autoregressive time series with a unit root. *Journal of the American statistical association*, 74(366a), 427-431.
- Phillips, P. (1988). Testing for unit roots in time series regression. *Biometrika*, 71, 599-607.
- Johansen, S., & Juselius, K. (1990). Maximum likelihood estimation and inference on cointegration—with applications to the demand for money. *Oxford Bulletin of Economics and statistics*, 52(2), 169-210.
- Pesaran, M. H., Shin, Y., & Smith, R. J. (2001). Bounds testing approaches to the analysis of level relationships. *Journal of applied econometrics*, 16(3), 289-326.
- Narayan, P. K. (2005). The saving and investment nexus for China: evidence from cointegration tests. *Applied economics*, 37(17), 1979-1990.
- Granger, C. W. J. (2001). Investigating causal relations by econometric models and cross-spectral methods. In *Essays in econometrics: collected papers of Clive WJ Granger* (pp. 31-47).
- Gomez-Gonzalez, J. E., Hirs-Garzon, J., & Uribe Gil, J. M. (2020). Global effects of US uncertainty: real and financial shocks on real and financial markets. IREA–Working Papers, 2020, IR20/15.
- Koop, G., Pesaran, M. H., & Potter, S. M. (1996). Impulse response analysis in nonlinear multivariate models. *Journal of econometrics*, 74(1), 119-147.

BIOGRAPHIES



Lotfi Saidi received the Ph.D. degree in electrical engineering from the University of Tunis, Tunisia, in 2014, and the Habilitation à Diriger des Recherches (HDR) degree in 2021 from the same University. He is an Associate Professor at the University of Sousse, Tunisia, and the head of the electronics and computer engineering department from 2017 to 2024, he is also an affiliated member of the Institut de Recherche Dupuy de Lôme (UMR CNRS 6027), Brest, France. Dr. Saidi is an IEEE Senior Member and his research interests include the application of advanced signal processing tools for electrical machines condition monitoring; prognosis and health management (PHM) of power converters; PHM of batteries; electrical systems' remaining useful life prediction, and energy management systems in microgrids and renewable energy applications.



Eric Bechhoefer received the B.S. degree in biology from the University of Michigan, Ann Arbor, the M.S. degree in operations research from the Naval Postgraduate School, Monterey, CA, and the Ph.D. degree in general engineering from Kennedy Western University, Cheyenne, WY. He is a former Naval Aviator who has extensively involved in condition-based

maintenance, rotor track and balance, vibration analysis of rotating machinery, and fault detection in electronic systems. He is currently with NRG Systems, Hinesburg, VT., Dr. Bechhoefer is a board member of the Prognostics Health Mangement Society (GPMS), and a member of the IEEE Reliability Society.



Mohamed Benbouzid completed his Ph.D. in electrical at the National Polytechnic Institute of Grenoble, Grenoble, France, in 1994. He further earned his Habilitation à Diriger des Recherches degree from the University of Amiens, Amiens, France, in 2000.

Following the completion of his Ph.D., Dr. Benbouzid joined the University of Amiens, where he held the position of Associate Professor in electrical engineering. Since

September 2004, he has been affiliated with the University of Brest, Brest, France, where he currently serves as a Full Professor in electrical engineering.

Prof. Benbouzid primary research interests and expertise include control of electric machines, variable-speed drives for traction, propulsion, and renewable energy applications, and fault diagnosis of electric machines.

Prof. Benbouzid is an IEEE Fellow and a Fellow of the IET. He is the Editor-in-Chief of the International Journal on Energy Conversion and the Applied Sciences (MDPI) Section on Electrical, Electronics and Communications Engineering. He is a Deputy Editor for the IET Renewable Power Generation.